



Localized mRNA translation and protein association

Downloaded from: <https://research.chalmers.se>, 2025-12-09 01:51 UTC

Citation for the original published paper (version of record):

Zhdanov, V. (2014). Localized mRNA translation and protein association. Central European Journal of Physics, 12(8): 603-609. <http://dx.doi.org/10.2478/s11534-014-0486-3>

N.B. When citing this work, cite the original published paper.

Localized mRNA translation and protein association

Short Communication

Vladimir P. Zhdanov^{1,2*}

*1 Section of Biological Physics, Department of Applied Physics,
Chalmers University of Technology, S-41296 Göteborg, Sweden*

2 Boreskov Institute of Catalysis, Russian Academy of Sciences, Novosibirsk 630090, Russia

Received 14 December 2013; accepted 14 May 2014

Abstract: Recent direct observations of localization of mRNAs and proteins both in prokaryotic and eukaryotic cells can be related to slowdown of diffusion of these species due to macromolecular crowding and their ability to aggregate and form immobile or slowly mobile complexes. Here, a generic kinetic model describing both these factors is presented and comprehensively analyzed. Although the model is non-linear, an accurate self-consistent analytical solution of the corresponding reaction-diffusion equation has been constructed, the types of localized protein distributions have been explicitly shown, and the predicted kinetic regimes of gene expression have been classified.

PACS (2008): 87.16.-b, 05.10.-a

Keywords: subcellular processes • gene transcription • mRNA translation • protein diffusion, association and degradation

© Versita Sp. z o.o.

1. Introduction

In cells, genes are transcribed by polymerases into mRNAs and ncRNAs. mRNAs are in turn translated by ribosomes into proteins. Understanding of the mechanisms and interplay of these processes is of great interest from different perspectives, and this truly interdisciplinary area has long attracted attention of biologists, chemists and physicists. Chemically, transcription and translation represent complex catalytic reactions. Due to abundant feedbacks and nonlinear substeps including, e.g., protein-mediated regulation of transcription or protein association, the corresponding kinetics often exhibit interesting non-

trivial features. Analysis of these features is a prerogative of chemical kinetics and statistical physics.

From the perspective of chemical engineering, a cell can be viewed as a reactor operating on the μm scale. How to describe such a reactor depends on the ratio of the time scales of reactions and reactant diffusion. Referring to the Stokes-Einstein hydrodynamic model of diffusion in solution, the diffusion of RNAs and proteins is usually assumed to be rapid, and accordingly these species are believed to be well stirred. Under such conditions, the kinetics of gene expression in a cell are described by using temporal equations (or the corresponding Monte Carlo simulations) for RNA and protein populations (or average concentrations) of the whole cell or its compartments including, e.g., the nucleus and cytoplasm. This approach also forms a basis for analysis of genetic networks in ensembles of cells with intercellular communication. The

*E-mail: zhdanov@catalysis.ru

kinetic models of this category are abundant (see, e.g., recent reviews, focused on stochastic effects [1], oscillations [2], ncRNAs [3], and complex genetic networks [4]).

With current advances in imaging capabilities allowing one to track macromolecules, it has become clear that mRNAs and proteins can be localized in different regions both in prokaryotic and eukaryotic cells. In eukaryotic cells, as one might expect, the localization is often related to various compartments. Prokaryotic cells, e.g., bacteria are not divided into compartments and their size is relatively small. Under such conditions, the localization (see recent studies focused on mRNAs [5–9] and proteins [9, 10] and the corresponding reviews [11–13] and [13–15], respectively) is what one would hardly expect. The regions of localization in bacteria are surprising diverse. In particular, localization of RNAs was observed near the cell poles, around the cell circumference, within the cytoplasm (helix-like patterns), and in foci near the transcribed genes [13]. Proteins were found to be localized in the same regions and also in association with membranes and membraneless organelles [13–15]. The resemblance between the spatial arrangements of mRNAs and proteins indicates that there seem to be some common general underlying principles behind localization of these species [13].

Although the mechanistic details of mRNA and protein localization are often obscure, some general concepts are discussed here. (i) In eukaryotic cells, as already noted, the localization is often related to compartments. (ii) In prokaryotic and eukaryotic cells, the localization may be directly or indirectly related to association with membranes or organelles. The corresponding “diffusion-and-capture” mechanism implies that a protein or RNA diffuses until it encounters its binding site [14]. (iii) Concerning bacteria, one can note that despite the absence of compartments, their structure is heterogeneous, and proteins (or RNAs) can be excluded or enriched at positions like the nucleoid or pole [17]. According to (ii) and (iii), the rate of RNA or protein diffusion is not of central importance, because the factors behind localization are related to thermodynamics. (iv) Two other general factors behind protein and RNA localization appear to be slow diffusion of these species (due to macromolecular crowding [16, 17]) and the ability of some mRNAs and/or proteins to aggregate and form immobile or slowly mobile complexes [11, 14].

Concerning protein and RNA diffusion, experiments indicate that this process in bacteria is usually somewhat slower than in eukaryotic cells, because bacteria are more crowded (especially near DNA) [17]. Diffusion in the latter cells is in turn appreciably slower than that in diluted aqueous solutions. Typical values of the diffusion coefficients of proteins in bacteria are $5 \times 10^{-9} - 10^{-7} \text{ cm}^2/\text{s}$ [17, 18]. Compared to proteins, mRNAs are less com-

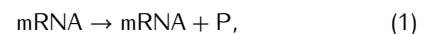
pact and their diffusion coefficients are often smaller, $(0.3 - 1) \times 10^{-9} \text{ cm}^2/\text{s}$ [16]. The rate of diffusion in cells depends not only on size but also on the specifics of the structure of species and cell physiological state. With increasing size, the diffusion coefficient usually decreases faster than one would expect according to the Stokes-Einstein model [17]. Using the typical values of protein and RNA diffusion coefficients and degradation rate constants (for the latter, see, e.g., [3]), one can conclude that the distribution of these species in bacteria should be homogeneous. This conclusion seems to be applicable to many but not to all proteins and RNAs. The observations of mRNA and protein localization in bacteria near the transcription region [7, 9] clearly indicate that the effective diffusion coefficients of some of mRNA and proteins may be appreciably smaller than on average.

Experimental studies of subcellular localization of RNAs and proteins have induced the development of spatio-temporal models of gene expression. A few available models are focused on protein aggregation and nucleoid occlusion [19–21]. Protein localization near the transcription region was described as a consequence of diffusion within and exchange between the condensed chromosomal DNA and an extrachromosomal area [9, 22]. There are treatments implying slow mRNA and protein diffusion and focused on the simplest scheme of mRNA and protein synthesis [23] and the formation of protein, playing a role of a transcription factor [24] (the kinetic equations used there are linear and accordingly can be solved analytically). Oscillatory spatio-temporal kinetics of gene expression were also analyzed [25, 26].

In this communication, we focus on a generic model describing localized mRNA translation and protein association and degradation, with slow protein diffusion. Although the corresponding reaction-diffusion equation is non-linear and cannot be exactly solved analytically, we construct an accurate self-consistent analytical solution and clarify what may happen in this case. To our knowledge, this is the first complete quantitative treatment of non-linear kinetics of gene expression with mRNA and protein localization.

2. Reaction steps

The model we use includes transcription of mRNA into protein,



reversible protein association resulting in the formation of dimers,



and degradation of monomeric and dimeric forms of protein,



Steps (1) and (3) are standard in gene expression. Formation of dimers (2) is often observed in cells and may serve as the first step of protein aggregation [11, 14].

In our analysis, the mRNA transcripts are considered to be localized in a certain place in a cell (e.g., due to their attachment to or near the cognate encoding gene [13]), and accordingly the protein synthesis [step (1)] occurs there as well. Our attention is primarily focused on the case of relatively slow P and B diffusion so that these species are distributed near the P source (as, e.g., observed in [9]). To show the specifics of this regime of gene expression, we first outline how the reaction is described in the well-stirred case and then comprehensively analyze the kinetics with localization of reactants.

As noted above, each step of our model and the key assumption that P and B diffuse slowly and accordingly can be localized are supported by experimental data. The validation is based, however, on experiments performed in different cells with different species. The latter is inevitable because the detailed experimental studies of mRNA and protein localization are now not numerous. For this reason, introducing our model, we do not try to indicate explicitly a system (cell and specific mRNA and protein) where it can be used.

3. Kinetics under well-stirred conditions

If P and B diffuse rapidly and are uniformly distributed in the cell, the reaction kinetics can be described in terms of average P and B concentrations, $c(t)$ and $C(t)$, as

$$dc/dt = w/V - 2\nu_a c^2 + 2\nu_d C - kc, \quad (5)$$

$$dC/dt = \nu_a c^2 - \nu_d C - \kappa C, \quad (6)$$

where w is the mRNA translation rate, ν_a and ν_d are the protein association and dissociation rate constants, k and κ are the protein degradation rate constants, and V is the cell volume.

In the steady-state case with $dc/dt = dC/dt = 0$, Eqs. (5) and (6) are read as

$$2\nu_a c^2 - 2\nu_d C + kc = w/V, \quad (7)$$

$$\nu_a c^2 - \nu_d C - \kappa C = 0. \quad (8)$$

The latter equation yields

$$C = \nu_a c^2 / (\nu_d + \kappa). \quad (9)$$

This expression can be rewritten as

$$C = \nu c^2 / 2\kappa, \quad (10)$$

where

$$\nu = 2\kappa\nu_a / (\nu_d + \kappa) \quad (11)$$

is the effective rate constant of P degradation via the association channel. Substituting (9) into (7) and using (11) yields

$$\nu c^2 + kc = w/V. \quad (12)$$

The solution of this equation is

$$c = \left(\frac{k^2}{4\nu^2} + \frac{w}{\nu V} \right)^{1/2} - \frac{k}{2\nu}. \quad (13)$$

The corresponding expression for C can be obtained by substituting (13) into (10).

To explain the physics behind expressions (13) and (10) for c and C , we introduce the maximum possible steady-state P and B concentrations,

$$c_o = w/kV, \quad C_o = w/2\kappa V, \quad (14)$$

and a dimensionless parameter defined as

$$p = k^2 V / 2\nu w. \quad (15)$$

The concentrations c_o and C_o cannot be reached simultaneously. The former concentration corresponds to the situation when the protein degradation occurs primarily via channel (3). The latter concentration is in turn for the situation when the protein degradation occurs primarily via channel (4). The physical meaning of p becomes clear noting that w/k is the scale of P population [provided that the protein degradation via channel (3) dominates or is comparable to the degradation via the channel including P association], w/kV is the scale of P concentration, $\nu w/kV$ is the scale of inverse time of P degradation via association, and k is the scale of inverse time of conventional P degradation. Thus, p represents the ratio of time scales characterizing two degradation channels.

With c_o , C_o and p , the expressions for c and C can be rewritten as

$$c = c_o[(p^2 + 2p)^{1/2} - p], \quad (16)$$

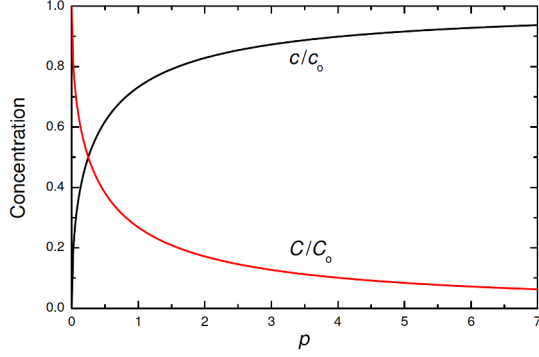


Figure 1. Normalized average P and B concentrations, c/c_0 and C/C_0 , as a function of p ($p \equiv k^2 V/2vw$) under well-stirred conditions according to Eqs. (16) and (17). With increasing p , the relative role of the conventional P degradation increases, P association becomes less efficient, and accordingly C/C_0 decreases.

$$C = C_0[(p+2)^{1/2} - p^{1/2}]^2/2. \quad (17)$$

Thus, the dependence of c and C on various parameters is consolidated in the dependence on p (Fig. 1). If $p \gg 1$, the protein degradation occurs primarily via channel (3), and expressions (16) and (17) are reduced to

$$c \simeq c_0 = w/kV, \quad (18)$$

$$C \simeq C_0/2p = \frac{vw^2}{2\kappa k^2 V^2}. \quad (19)$$

If $p \ll 1$, the protein degradation occurs primarily via the channel including P association, and one has

$$c \simeq (2p)^{1/2} c_0 = (w/vV)^{1/2}, \quad (20)$$

$$C \simeq C_0 = w/2\kappa. \quad (21)$$

As already noted, Eqs. (18)–(21) indicate that c reaches c_0 provided that $p \gg 1$, while C reaches C_0 at $p \ll 1$.

4. Kinetics with localization of reactants

If P and B diffuse slowly and are localized near the mRNA-translation region, the reaction kinetics can be described using the reaction-diffusion equations for r - and t -dependent P and B concentrations, $c(r, t)$ and $C(r, t)$. Assuming the mRNA translation to occur at $r = 0$, we have

$$\partial c/\partial t = D\nabla^2 c - 2v_a c^2 + 2v_d C - kc + w\delta(r), \quad (22)$$

$$\partial C/\partial t = \mathcal{D}\nabla^2 C + v_a c^2 - v_d C - \kappa C, \quad (23)$$

where D and \mathcal{D} are the P and B diffusion coefficients, and $\delta(r)$ is the delta function (the other designations are as in Eqs. (5) and (6)). Using these equations, we do not take explicitly into account that the cell is heterogeneous and P and B may reversibly attach to numerous sites (e.g. at DNA) with small binding energy. The P and B populations of such sites can usually be expressed via c and C , respectively. Following this line, one can take the cell heterogeneity into account and derive Eqs. (22) and (23) by redefining the degradation rate constants. Thus, in fact, Eqs. (22) and (23) may remain valid.

In our analysis, we focus on the steady-state case with $\partial c/\partial t = \partial C/\partial t = 0$. Under these conditions corresponding to typical experiments mentioned in the Introduction, P and B concentrations, $c(r)$ and $C(r)$, depend only on r . Noticing that B size is larger than P size, we consider that due to macromolecular crowding the B diffusion coefficient is appreciably smaller than the P diffusion coefficient, and accordingly B diffusion is negligible. This approximation is acceptable because with increasing size, as already noted in the Introduction, the diffusion coefficient usually decreases faster than one could expect according to the Stokes-Einstein model [17]. In addition, aggregated proteins are often misfolded and due to this factor their diffusion rate may be low. Under these conditions, Eqs. (22) and (23) are read as

$$\frac{D}{r^2} \frac{d}{dr} r^2 \frac{dc}{dr} - 2v_a c^2 + 2v_d C - kc = 0, \quad (24)$$

$$v_a c^2 - v_d C - \kappa C = 0. \quad (25)$$

Near the P source, the boundary condition for Eq. (24) is

$$-4\pi r^2 D \left. \frac{dc}{dr} \right|_{r \rightarrow 0} = w. \quad (26)$$

Concerning the other boundary conditions, we consider that slow diffusion results in P and B localization in a small region inside the cell. Outside this region, P and B concentrations are negligible, and accordingly the restrictions on diffusion related to the outer cellular membrane are negligible as well. Under such circumstances, Eqs. (24) and (25) can be solved in the whole space, assuming that there are no limitations on diffusion at $r \rightarrow \infty$.

According to (25), we have

$$C = \frac{v_a c^2}{v_d + \kappa} \equiv \frac{v c^2}{2\kappa}, \quad (27)$$

where v is defined by (11). This expression for C is similar to expressions (9) and (10). The only difference is that C

in (27) is considered to depend on r , while expressions (9) and (10) contain the average concentration. Substituting (27) into (24) yields

$$\frac{D}{r^2} \frac{d}{dr} r^2 \frac{dc}{dr} - \nu c^2 - kc = 0. \quad (28)$$

This non-linear equation cannot be exactly solved analytically. To construct an accurate approximation, we note that νc^2 and kc represent the rates of two channels of P degradation occurring via association [(2) and (4)] and directly (3), respectively. Comparing these rates, we see that νc plays the same role as k , i.e., νc plays the role of a rate constant. To solve Eq. (28), we replace νc by the effective rate constant k_* , which is calculated self-consistently as described below. Thus, we replace Eq. (28) by

$$\frac{D}{r^2} \frac{d}{dr} r^2 \frac{dc}{dr} - k_* c - kc = 0. \quad (29)$$

The solution of the latter equation is

$$c(r) = \frac{w \exp(-\alpha r)}{4\pi D r}, \quad (30)$$

where $\alpha = [(k + k_*)/D]^{1/2}$.

To express k_* via the model parameters, we note that according to Eq. (29) the integral P degradation rate via association [(2) and (4)] is $\int_0^\infty k_* c(r) 4\pi r^2 dr$. According to Eq. (28), on the other hand, this rate is $\int_0^\infty \nu c(r)^2 4\pi r^2 dr$. Eq. (28) can be replaced by Eq. (29) provided these two rates are equal,

$$\int_0^\infty k_* c(r) 4\pi r^2 dr = \int_0^\infty \nu c(r)^2 4\pi r^2 dr. \quad (31)$$

Substituting (30) into (31), we obtain

$$k_* = \frac{\nu w \alpha^3}{8\pi(k + k_*)}. \quad (32)$$

This equation for k_* can be rewritten as

$$k_*/k = 2\rho(1 + k_*/k)^{1/2}, \quad (33)$$

where

$$\rho = \frac{\nu w}{16\pi k^{1/2} D^{3/2}} \quad (34)$$

is a dimensionless parameter. Solving Eq. (33), we have

$$k_*/k = [\rho + (\rho^2 + 1)^{1/2}]^2 - 1. \quad (35)$$

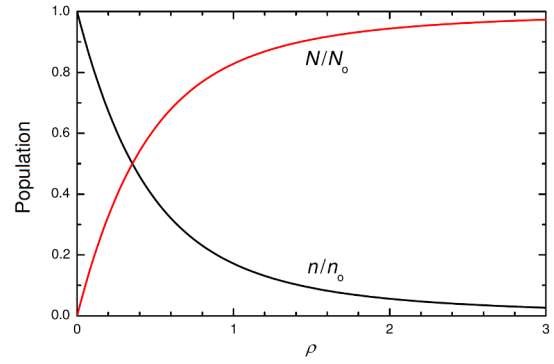


Figure 2. Normalized P and B populations, n/n_0 and N/N_0 , as a function of ρ ($\rho \equiv \nu w/16\pi k^{1/2} D^{3/2}$) in the case of localization near the transcribed gene (according to Eqs. (36) and (37)). With increasing ρ , the relative role of the conventional P degradation decreases, P association becomes more efficient, and accordingly N/N_0 increases.

Using expression (30) for c and expression (27) for C , we can now calculate P and B populations,

$$n = \int_0^\infty c(r) 4\pi r^2 dr = \frac{n_0}{1 + k_*/k}, \quad (36)$$

$$N = \int_0^\infty C(r) 4\pi r^2 dr = \frac{2\rho N_0}{(1 + k_*/k)^{1/2}}, \quad (37)$$

where $n_0 \equiv w/k$ and $N_0 \equiv w/2k$ are their maximum values [these values are similar to those obtained earlier (14) under well-stirred conditions]. Taking into account that the ratio k_*/k depends only on ρ (Eq. (35)), we conclude that in fact the dependence of n and N on various parameters is reduced the dependence on ρ (Fig. 2).

Expressions (27), (30) and (34)–(37), determining P and B distributions and total populations, are central in our study. To confirm the accuracy of the self-consistent approximation used to derive these expressions, we have calculated $c(r)$ by integrating Eq. (24) numerically in a broad range of ρ (from 0.01 to 10). Comparing the results of numerical integration with those predicted analytically by Eq. (30) (Fig. 3) indicates that the analytical solution is fairly accurate in the whole localization region even at large ρ .

Employing expressions (34)–(37), we can classify the regimes of gene expression. To make the classification less formal, it is instructive to scrutinize the physical meaning of the dimensionless parameter ρ determined by (34), which can be rewritten as

$$\rho = \frac{\nu w}{16\pi k^2 (D/k)^{3/2}}. \quad (38)$$

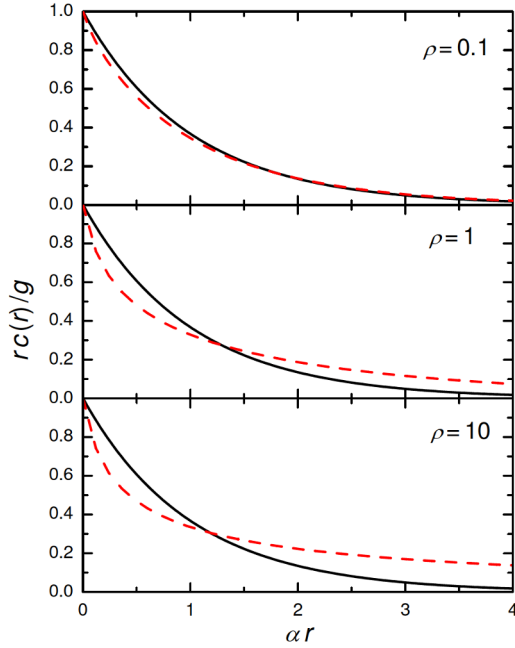


Figure 3. P distribution, multiplied by r and normalized to g ($g \equiv w/4\pi D$), as a function of r for $\rho = 0.01, 1$, and 10 . The solid and dashed lines correspond to expression (30) and numerical integration of Eq. (24), respectively. The analytical solution is seen to be rather accurate.

Taking into account that $2(D/k)^{1/2}$ is the length scale of the region where the processes under consideration takes place [provided the rate of protein degradation via channel (3) is higher or comparable to that via the channel that includes P association], we notice that $8(D/k)^{3/2}$ represents the scale of the volume of this region. In turn, w/k is the scale of protein population, $w/[8k(D/k)^{3/2}]$ is the scale of protein concentration, $\nu w/[8k(D/k)^{3/2}]$ is the scale of inverse time of protein degradation via association, and k is the scale of inverse time of conventional protein degradation. Thus, in analogy with (15), ρ represents the ratio of the time scales characterizing the two degradation channels.

If $\rho \ll 1$, the protein degradation occurs primarily via channel (3), and expressions (35)–(37) yield $k_*/k \simeq 2\rho \ll 1$, and

$$n \simeq n_o = w/k, \quad (39)$$

$$N \simeq 2\rho N_o = \frac{\nu w^2}{16\pi k^{1/2} D^{3/2}} \ll N_o. \quad (40)$$

If $\rho \gg 1$, the protein degrades primarily via the channel that includes P association, and expressions (35)–(37) result in $k_*/k \simeq 4\rho^2 \gg 1$, and

$$n \simeq k n_o / k_* = w/k_* \ll n_o, \quad (41)$$

$$N \simeq N_o = w/2\kappa. \quad (42)$$

To complete our analysis, we note that we have used the delta function in Eq. (22) in order to describe the mRNA distribution. Thus, expression (30) for c and the corresponding expression for C represent Green functions. For an arbitrary mRNA distribution, $f(r)$, P and B distributions can thus be obtained by convolution. For example, the P distribution is

$$c(r) = \int f(r') \frac{w \exp(-\alpha|r-r'|)}{4\pi D|r-r'|} d^3 r'. \quad (43)$$

Such integrals can be calculated analytically (see, e.g., [23]) or numerically. Physically, it is clear that with this modification P and B will be distributed more or less uniformly in the region of mRNA localization while outside this region the distribution will be explicitly described by expression (30) for c and the corresponding expression for C .

The model we used contains many kinetic parameters. To present the results of our analysis in a compact form, we have widely employed dimensionless combination of parameters. Concerning specific parameters, we recall typical values of the rates or rate constants of transcription (less than or about $1\text{--}10 \text{ min}^{-1}$), translation (less than or about $1\text{--}10 \text{ min}^{-1}$), and mRNA and protein degradation (less than or about $0.01\text{--}0.1 \text{ min}^{-1}$) [3, 27]. The rate of protein association (2) is limited by diffusion, $\nu_a \leq 2\pi D a$ (a is the protein size), and accordingly the corresponding rate constant is less than $10^{-11} \text{ cm}^3/\text{min}$, while the dissociation rate constant is typically much less than 10^8 min^{-1} .

5. Conclusion

Recent direct observations of localization mRNAs and proteins both in prokaryotic and eukaryotic cells [5]–[15] is one of the most most exciting breakthroughs in molecular cellular biology. Among other factors, such observations can be related to slow mRNA and/or protein diffusion and the ability of some of mRNAs and/or proteins to aggregate and form immobile or slowly mobile complexes [11, 14]. We have presented and comprehensively analyzed a generic model describing these two factors. In particular, our model includes protein association resulting in dimer formation (this is the first step of protein aggregation). Although the model is non-linear, we have constructed an accurate self-consistent analytical solution of the corresponding reaction–diffusion equation. Using the analytical results, we have clarified and classified the possible kinetic regimes and have explicitly shown the types of localized protein distributions.

The corresponding kinetics under well-stirred conditions have been analyzed as well. To some extent, the kinetics with reactant localization are similar to those predicted under well-stirred conditions. In both cases, the protein degradation may occur primarily either directly or via association. The criteria for transition from one regime to another are, however, different. In particular, the condition for transition depends on the value of p (15) in the former case and on the value of ρ (38) in the latter case. The key difference is that p is independent of D while ρ is inversely proportional to $D^{3/2}$. With decreasing D , ρ becomes larger, and B population increases (Fig. 2), because localization of P increases and the rate of association increases as well.

The results obtained help to understand the type of localization of proteins in situations where the protein synthesis is accompanied by their aggregation. As an example of aggregation, our model includes dimer formation. The formation of trimers and other multimers can easily be described in analogy provided their diffusion is negligible. In chemistry, various kinetic schemes of protein aggregation were widely treated under well-stirred conditions [28]. If, for example, the aggregation steps are irreversible (as in the Lumry-Eyring model [28, 29]), one can express the concentration of dimers and multimers via concentration of monomers and, in our context, use Eq. (28). Although our analysis is focused on gene expression, the results obtained may be useful in a broader context, because our model describes the simplest scheme of aggregation and degradation of particles with a localized source of monomers.

References

- [1] J. Rausenberger, C. Fleck, J. Timmer, M. Kollmann, *Progr. Biophys. Molec. Biol.* 100, 57 (2009)
- [2] O. Purcell, N.J. Savery, C.S. Grierson, M. di Bernardo, *J. Roy. Soc. Interface* 7, 1503 (2010)
- [3] V.P. Zhdanov, *Phys. Rep.* 500, 1 (2011)
- [4] D.F.T. Veiga, B. Dutta, G. Balazsi, *Molec. Biosyst.* 6, 469 (2010)
- [5] M. Valencia-Burtona et al., *Proc. Natl. Acad. Sci. USA* 106, 16399 (2009)
- [6] J.H. Russell, K.C. Keiler, *Proc. Natl. Acad. Sci. USA* 106, 16405 (2009)
- [7] P. Montero Llopis, A.F. Jackson, O. Sliusarenko, I. Surovtsev, J. Heinritz, T. Emonet, C. Jacobs-Wagner, *Nature* 466, 77 (2010)
- [8] K. Nevo-Dinur, A. Nussbaum-Shochat, S. Ben-Yehuda, O. Amster-Choder, *Science* 331, 1081 (2011)
- [9] T.E. Kuhlman, E.C. Cox, *Molec. Syst. Biol.* 8, 610 (2012)
- [10] G. Laloux, C. Jacobs-Wagner, *J. Cell Biol.* 201, 827 (2013)
- [11] N.E. Broude, *Molec. Microbiol.* 80, 1137 (2011)
- [12] K.C. Keiler, *Curr. Opin. Microbiol.* 14, 155 (2011)
- [13] K. Nevo-Dinur, S. Govindarajan, O. Amster-Choder, *Trends Genet.* 28, 314 (2012)
- [14] D.Z. Rudner, R. Losick, *Cold Spring Harb. Perspect. Biol.* 2, a000307 (2010)
- [15] E. Evguenieva-Hackenberg, V. Roppelt, C. Lassek, G. Klug, *RNA Biol.* 8, 49 (2011)
- [16] T. Misteli, *Histochem. Cell Biol.* 129, 5 (2008)
- [17] J.T. Mika, B. Poolman, *Curr. Opin. Biotechnol.* 22, 117 (2011)
- [18] M. Kumar, M.S. Mommer, V. Sourjik, *Biophys. J.* 98, 552 (2010)
- [19] S. Saberi, E. Emberly, *PLoS Comput. Biol.* 6, e1000986 (2010)
- [20] S. Saberi, E. Emberly, *PLoS One* 8, e64075 (2013)
- [21] A.-S. Coquel et al., *PLoS Comput. Biol.* 9, e1003038 (2013)
- [22] T.E. Kuhlman, E.C. Cox, *Phys. Rev. E* 88, 022701 (2013)
- [23] V.P. Zhdanov, *Cent. Eur. J. Phys.* 10, 533 (2012)
- [24] O. Pulkkinen, R. Metzler, *Phys. Rev. Lett.* 110, 198101 (2013)
- [25] V.P. Zhdanov, *Chem. Phys. Lett.* 458, 247 (2008)
- [26] P. Rashkov, B.A. Schmitt, L. Sogaard-Andersen, P. Lenz, S. Dahlke, *Bull. Math. Biol.* 74, 2183 (2012)
- [27] M. Kaern, T.C. Elston, W.J. Blake, J.J. Collins, *Nature Rev. Genet.* 6, 451 (2005)
- [28] A.M. Morris, M.A. Watzky, R.G. Finke, *Biochim. Biophys. Acta* 1794, 375 (2009)
- [29] C.J. Roberts, *J. Phys. Chem. B* 107, 1194 (2003)